Effects of self-steepening and self-frequency shifting on short-pulse splitting in dispersive nonlinear media

Marek Trippenbach and Y. B. Band
Departments of Chemistry and Physics, Ben-Gurion University of the Negev, Beer-Sheva 84105, Israel
(Received 5 November 1997; revised manuscript received 20 January 1998)

We characterize the propagation of short optical pulses through dispersive media with a cubic self-focusing nonlinear polarization, which incorporates self-steepening and self-frequency shifting. These effects can significantly affect pulse propagation dynamics, both in the normal but especially in the anomalous dispersion regimes. The nature of the dynamics is significantly different in the two regimes. [S1050-2947(98)09705-4]

PACS number(s): 42.65.Re, 42.65.Sf, 42.25.Fx

I. INTRODUCTION

Many recent studies have demonstrated that pulse splitting occurs in $\chi^{(3)}$ media for optical pulses with powers beyond the self-focusing threshold [1–4]. Here we show that self-steepening (SS) and self-frequency shifting (SFS) can suppress pulse splitting as it shocks the trailing edge of the pulse and introduces a low frequency spectral component for a pulse in the anomalous dispersion regime [where very narrow temporal features are created due to the interplay between group velocity dispersion (GVD) and self-focusing]. In the normal dispersion regime (where narrow temporal features are not produced), SS and SFS are significant effects only for extremely short input pulses; in this case SS and SFS do not suppress pulse splitting in time or transverse spatial dimensions; rather, a shock at the trailing edge of the pulse is initially produced, spatial and temporal pulse splitting occurs, eventually enhancement of the leading pulse results, and a high frequency tail and a low frequency spectral component are generated. The amplitude of the leading pulselet becomes larger than the trailing pulselet. SFS enhances the effects introduced by SS and also shifts the frequency of the pulse. The effects of SS have been well studied in one spatial dimension (i.e., optical fibers) [5–8] where the transverse spatial dimensions are eliminated due to transverse mode constraints. There it was shown that the effects of GVD to some extent wash out the shock front in both normal and anomalous dispersion regimes for 1D propagation (we shall see that in 3D, before pulse splitting occurs, the effects of the shock term are still readily apparent). Here we study the effects of SS and SFS for pulse propagation in bulk dispersive media where the transverse dimensions result in diffraction, a prominent aspect of the propagation. We consider the high intensity regime above the threshold for spatial pulse splitting [4]. Recall [4] that above the threshold for self-focusing, there are two separate thresholds for pulse splitting. The lower pulse splitting threshold is for temporal pulse splitting (for diffraction length smaller than dispersion length), wherein the pulse splits apart in time. The higher pulse splitting threshold is for temporal and spatial pulse splitting. We consider here energies above the second threshold (i.e., the spatial pulse splitting threshold). However, even for intensities above the temporal pulse splitting threshold but below the spatial pulse splitting threshold, SS and SFS can affect short pulse propagation dynamics in a similar way.

The propagation equation for the slowly varying envelope of the electric field (SVE), $\vec{A}(\vec{x},t)$, can be derived by differentiating it with respect to the position coordinate in the direction of the central wave vector $\vec{K}_0$, $\vec{s}_0=\vec{K}_0/|K_0|$, which we choose to be along the space-fixed z axis [4,9–11]. For linearly polarized light,

$$\frac{\partial A}{\partial z}=-\beta_1\frac{\partial A}{\partial t}-\frac{i}{2}\beta_2\frac{\partial^2 A}{\partial t^2}+\frac{1}{6}\beta_3\frac{\partial^3 A}{\partial t^3}+\frac{i}{2}\gamma_{xx}\left(\frac{\partial^2 A}{\partial x^2}+\frac{\partial^2 A}{\partial y^2}\right)+\frac{1}{3}\gamma_{txx}\left(\frac{\partial^3 A}{\partial x^2\partial t}+\frac{\partial^3 A}{\partial y^2\partial t}\right)+i\gamma_{\mathrm{NL}}|A|^2A-\gamma_{\mathrm{NL}}\omega_0^{-1}\partial(|A|^2A)/\partial t-i\gamma_{NL}\tau_R A\partial(|A|^2)/\partial t, \quad (1)$$

where $\gamma_{\mathrm{NL}}=2\pi\chi^{(3)}\omega_0/(n(\omega_0)c)$ and τ_R is the decay time of the Raman gain ($\tau_R\approx$ 5 fs). The last three terms on the right-hand side of Eq. (1) are the self-focusing $\chi^{(3)}$ nonlinear term, which gives rise to self-phase modulation (SPM), the self-steepening term, and the self-frequency shifting term, respectively. Here β_1 is the inverse group velocity, β_2 the group velocity dispersion, β_3 the third order dispersion, γ_{xx} the Fresnel diffraction coefficient, and γ_{txx} the coefficient of the mixed space-time third order term that accounts for the spherical nature of the wavefront surface of a pulse originating from a point source [10]. For a cylindrically symmetric pulse of width w_0, or for a pulse whose transverse y dimension is large and can therefore be ignored, Eq. (1) can be written in terms of the following lengths (the smaller the length, the more important the corresponding term in the PDE): diffraction length $L_{\mathrm{DF}}=\gamma_{xx}w_0^2/2=\pi w_0^2/\lambda_0$, where $\gamma_{xx}=c/(n(\omega_0)\omega_0)$, dispersion length $L_{\mathrm{DS}}=\tau_0^2/\beta_2$, third order dispersion length $L_{\mathrm{TOD}}=\tau_0^3/\beta_3$, third order dispersion-diffraction length, $L_{\mathrm{DSDF}}=\tau_0 w_0^2/\gamma_{txx}$, nonlinear length $L_{\mathrm{NL}}=(\gamma_{\mathrm{NL}}|A_0|^2)^{-1}$, where A_0 is the initial pulse peak amplitude, the SS length $L_{\mathrm{SS}}=\omega_0\tau_0(\gamma_{\mathrm{NL}}|A_0|^2)^{-1}$, and the SFS length $L_{\mathrm{SFS}}=(\tau_0/\tau_R)(\gamma_{\mathrm{NL}}|A_0|^2)^{-1}$. Clearly, as τ_0 decreases and $|A_0|^2$ increases, L_{SS} and L_{SFS} decrease (SS and SFS become more important). The propagation equation can be written explicitly in terms of these length scales as follows:

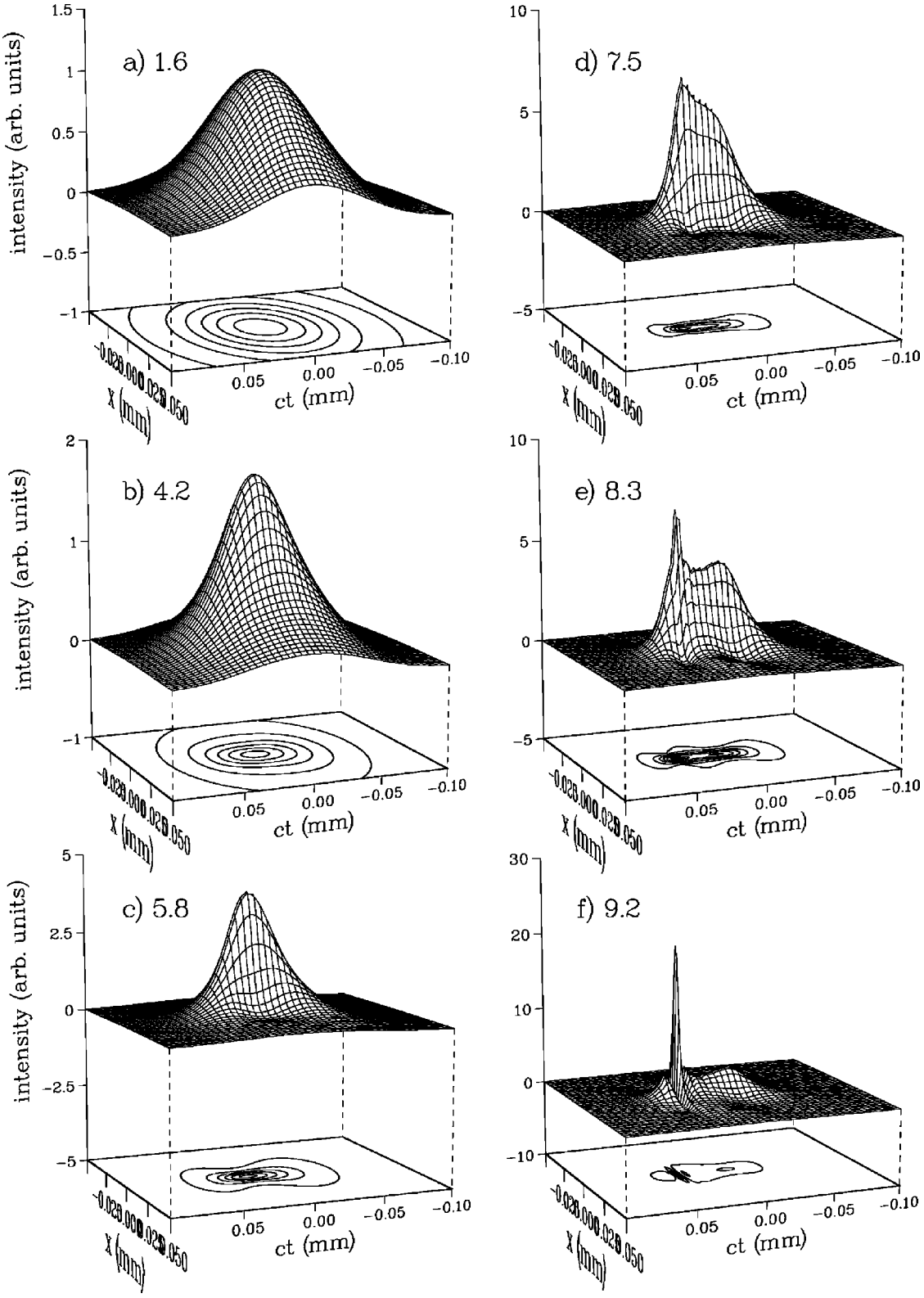

FIG. 1. Pulse intensity versus x and ct for various propagation distances L_z (in mm) as indicated next to the label, for the anomalous dispersion regime.

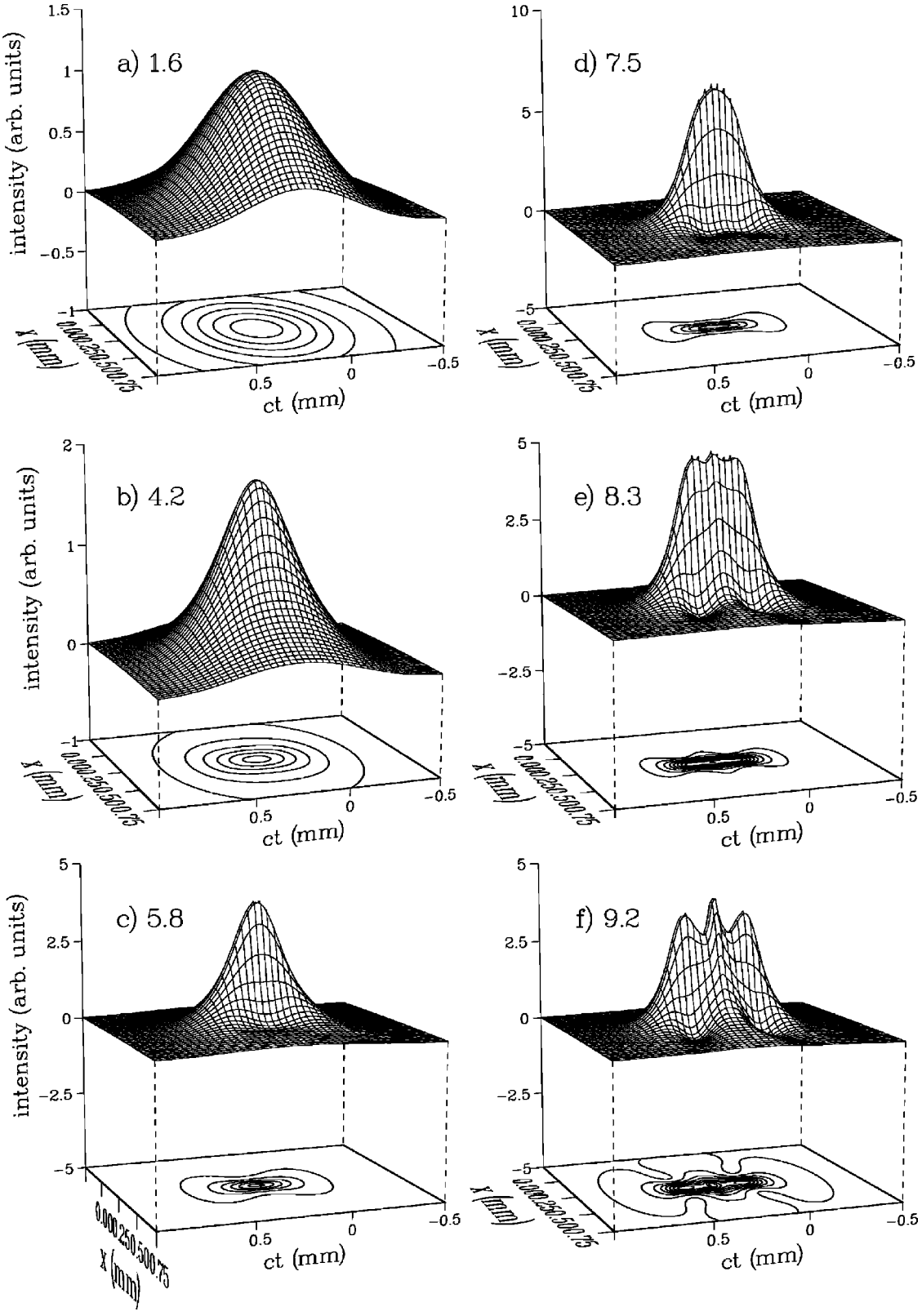

FIG. 2. Pulse intensity versus x and ct for various propagation distances L_z (in mm) as indicated next to the label, for the anomalous dispersion regime without SFS and SS.

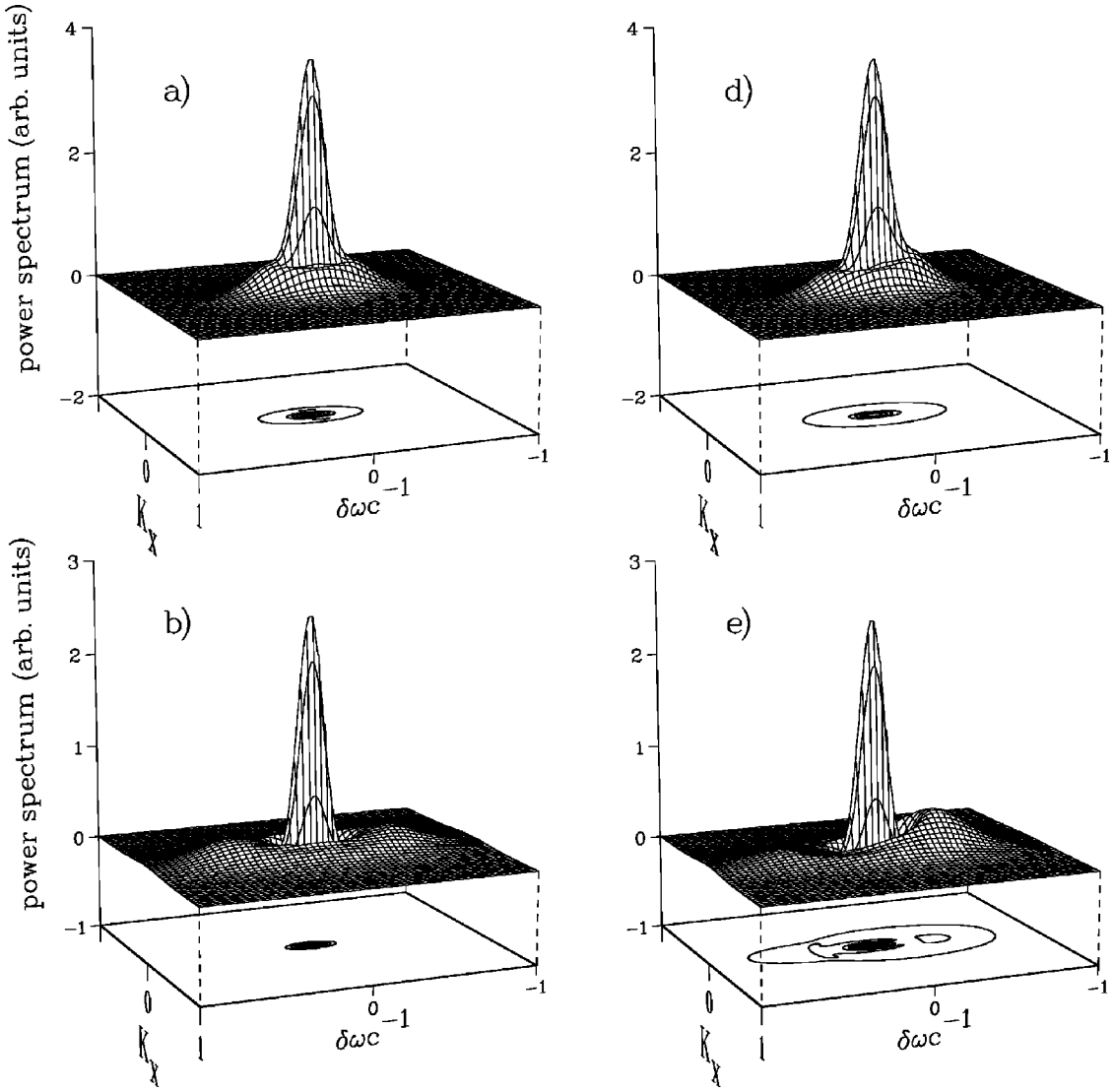

FIG. 3. Power spectrum versus $\delta\omega/c=(\omega-\omega_0)/c$ and K_x. (a) and (b) correspond to Figs. 1(b) and 1(d) and (c) and (d) (without SFS and SS) correspond to Fig. 2(a) and 2(d), respectively.

$$\frac{\partial A}{\partial z}=-i\frac{\tau_0^2}{L_{\mathrm{DS}}}\frac{\partial^2 A}{\partial t^2}+\frac{\tau_0^3}{L_{\mathrm{TOD}}}\frac{\partial^3 A}{\partial t^3}+i\frac{w_0^2}{L_{\mathrm{DF}}}\left(\frac{\partial^2 A}{\partial x^2}+\frac{\partial^2 A}{\partial y^2}\right)$$
$$+\frac{w_0^2\tau_0}{L_{\mathrm{DSDF}}}\left(\frac{\partial^3 A}{\partial x^2\partial t}+\frac{\partial^3 A}{\partial y^2\partial t}\right)+i\frac{1}{|A_0|^2L_{\mathrm{NL}}}|A|^2A$$
$$-\frac{\tau_0}{|A_0|^2L_{\mathrm{SS}}}\partial(|A|^2A)/\partial t-i\frac{\tau_0}{|A_0|^2L_{\mathrm{SFS}}}\partial(|A|^2)/\partial tA. \tag{2}$$

Here we have gone to a frame moving with the pulse (transforming $z\Rightarrow z-t/\beta_1$) to eliminate the β_1 term from the propagation equation. The relative importance of each of the terms in the equation is determined in inverse proportion to the size of the corresponding length scales.

In what follows we consider pulse propagation in silica (SiO_2). For presentation purposes, we take the y transverse width to be very large and plot $|A(x,z,t)|^2$ vs x and ct for various propagation distances L_z in the frame traveling with the group velocity, and the Fourier transform $|A(K_x,\omega)|^2$ versus $(\omega-\omega_0)/c$ and K_x.

II. ANOMALOUS DISPERSION REGIME

We choose the following pulse parameters in the anomalous dispersion regime: central wavelength $\lambda_0=1400$ nm, temporal pulse duration $\tau_0=66$ fs, initial spot size $w_0=40\lambda_0$ ($\approx 56\mu$m), and intensity 6.0×10^{10} W/cm^2. The length scales for these parameters are as follows: $L_{\mathrm{NL}}=2220\ \mu\mathrm{m}<L_{\mathrm{DF}}=7040\ \mu\mathrm{m}<L_{\mathrm{SFS}}=4.93\times10^4\ \mu\mathrm{m}<L_{\mathrm{SS}}=2.0\times10^5\ \mu\mathrm{m}<|L_{\mathrm{DS}}|=6.9\times10^5\ \mu\mathrm{m}<L_{\mathrm{DSDF}}=8.6\times10^5\ \mu$m ($L_{\mathrm{DS}}$ is negative since in the anomalous dispersion regime $\beta_2<0$). Figure 1 shows the pulse propagation dynamics as a function of L_z. The maximum propagation distance shown is $L_z=9.2\times10^3\ \mu$m, which is smaller than L_{SFS} and L_{SS}. Nevertheless, because of the decrease in the temporal duration of the pulse in the anomalous dispersion regime due to the interplay between GVD and SPM, and because the peak intensity of the pulse increases, the propagation distance over which SFS and SS become significant is actually

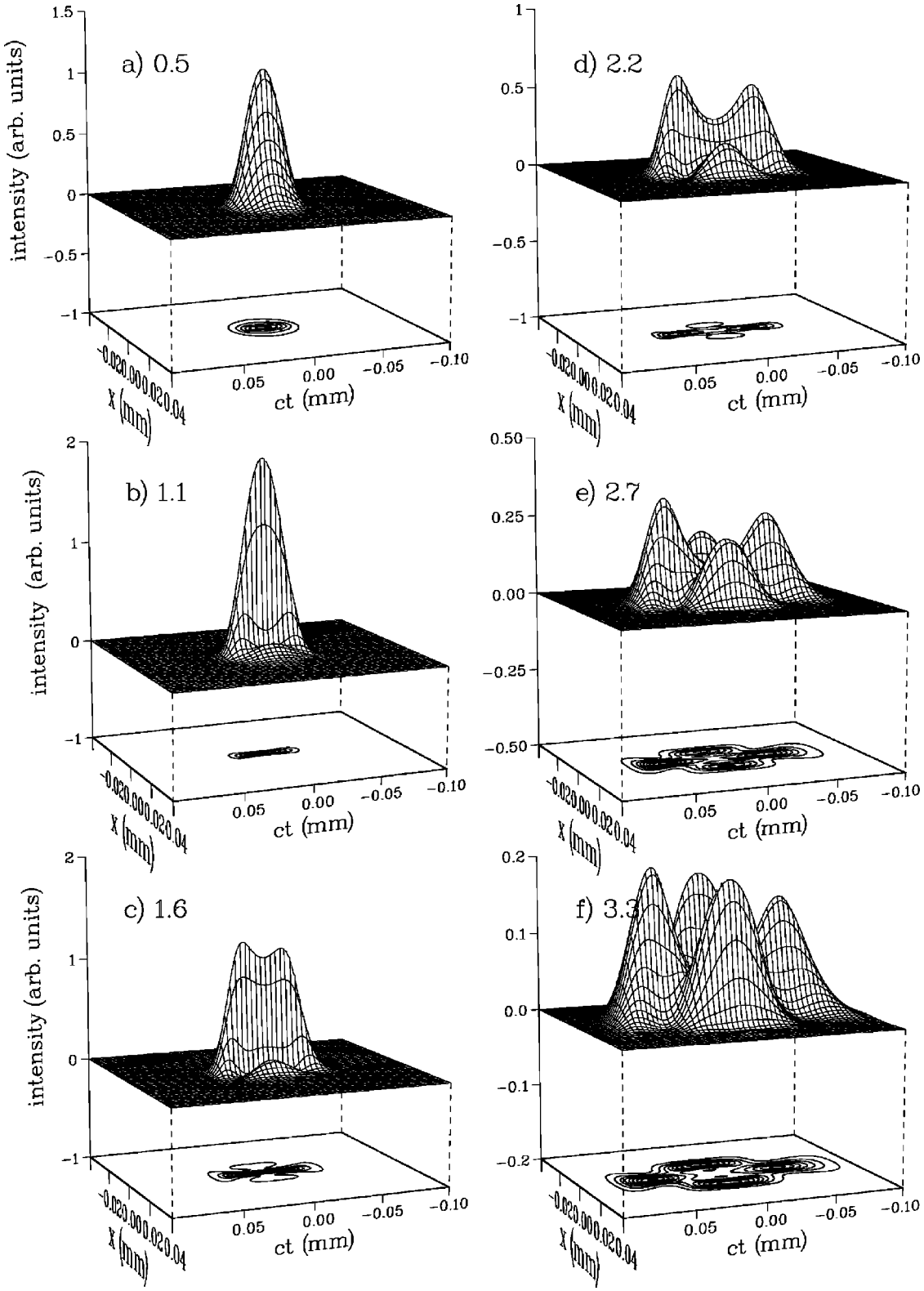

FIG. 4. Pulse intensity versus x and ct for various propagation distances L_z (in mm) for a very short pulse in the normal dispersion regime including only the SPM nonlinearity (without SFS and SS).

smaller than the estimates given by L_{SFS} and L_{SS}. Without SS and SFS (see Fig. 2), self-focusing of the pulse occurs, and eventually the pulse splits in time into three pulselets with the central peak having an extremely short pulse duration. This central peak ultimately splits apart in the transverse spatial dimension [11]. Upon including SS, the trailing edge of the pulse becomes shocked, the peak intensity of the pulse is increased, and the peak of the pulse moves towards the trailing edge of the pulse. SFS serves to transfer photons to lower frequency, and the lower frequency photons travel slower in the anomalous dispersion regime. Hence the leading edge of the pulse is suppressed relative to the trailing

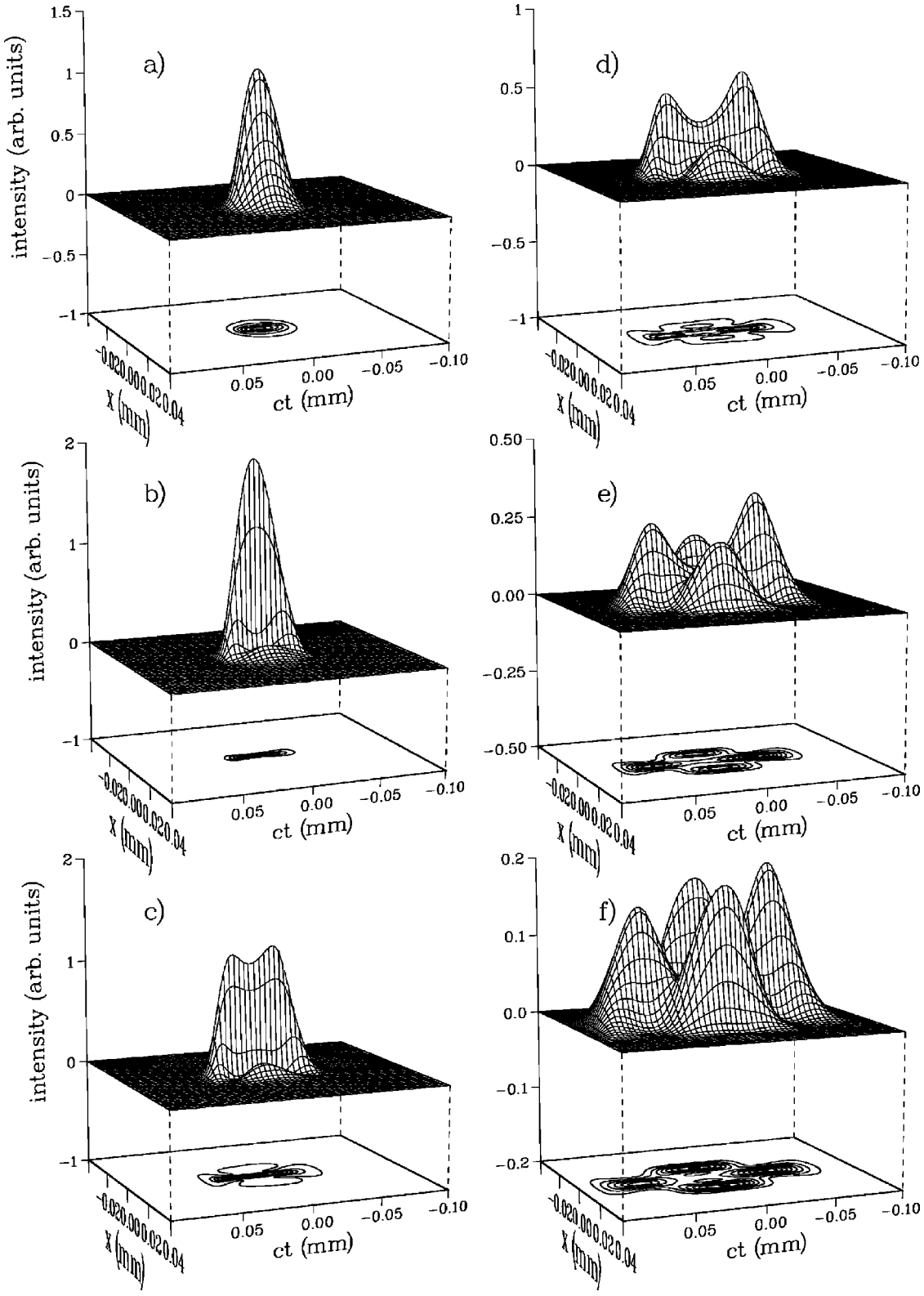

FIG. 5. Pulse intensity versus x and ct for various propagation distances L_z for a very short pulse in the normal dispersion regime without SFS (with SPM and SS). Propagation distances are the same as in Fig. 4.

edge of the pulse because of both SS and SFS. Pulse breakup following self-focusing of the incident pulse is therefore strongly suppressed.

Figures 3(a) and 3(b) show the power spectrum $|A(K_x,\omega)|^2$ corresponding to Fig. 1(b) and 1(d), respectively, and Figs. 3(c) and 3(d) correspond to Figs. 2(b) and Fig. 2(d). Without SS and SFS, a pedestal develops around the central peak in ω-K_x space. With SS and SFS, the pedestal becomes distorted, destroying the near symmetry (near because of the small TOD) around the central frequency, so that the lower frequency portion becomes more intense. The higher frequency feature, due to SS, is stretched over a wider

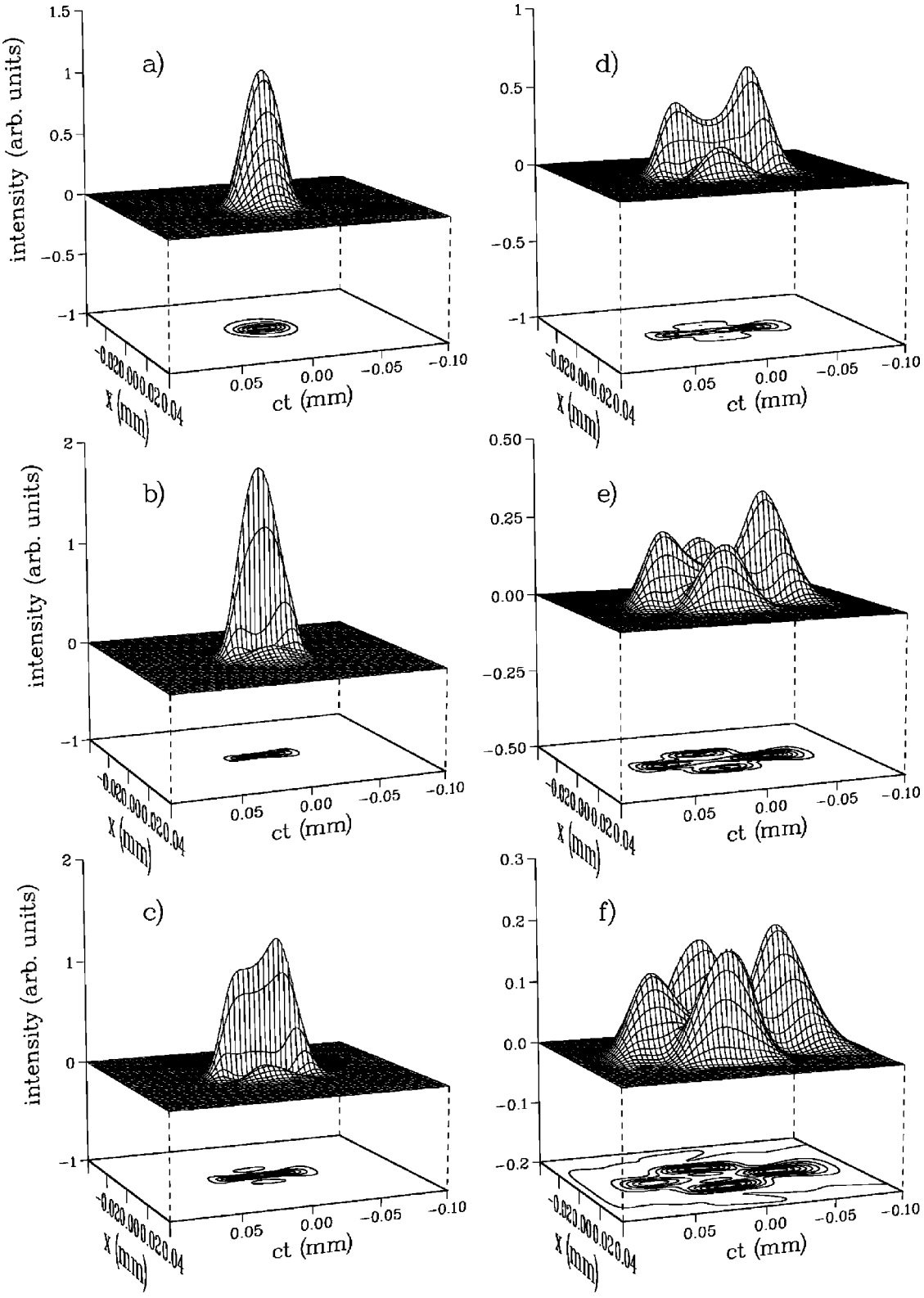

FIG. 6. Pulse intensity versus x and ct for various propagation distances L_z for a very short pulse in the normal dispersion regime without SS (with SPM and SFS). Propagation distances are the same as in Fig. 4.

spectral range and is less intense than the low frequency feature, due to SFS. This is analogous to the 1D case [5].

III. NORMAL DISPERSION REGIME

We now consider the normal dispersion regime and take $\lambda_0 = 800$ nm. We consider an extremely short pulse duration since only then we expect the effects of SFS and SS to be evident in this regime. We take $\tau_0 = 10$ fs (although qualitatively similar effects are present at 15 fs), $w_0 = 20\lambda_0 (16\ \mu\text{m})$, and an intensity of 9.75×10^{11} W/cm^2. The length scales are as follows: $L_{\text{NL}} = 333\ \mu\text{m} < L_{\text{DF}} = 1000\ \mu\text{m} < L_{\text{SFS}} = 1111\ \mu\text{m} < L_{\text{DS}} = 5511\ \mu\text{m} < L_{\text{SS}}$

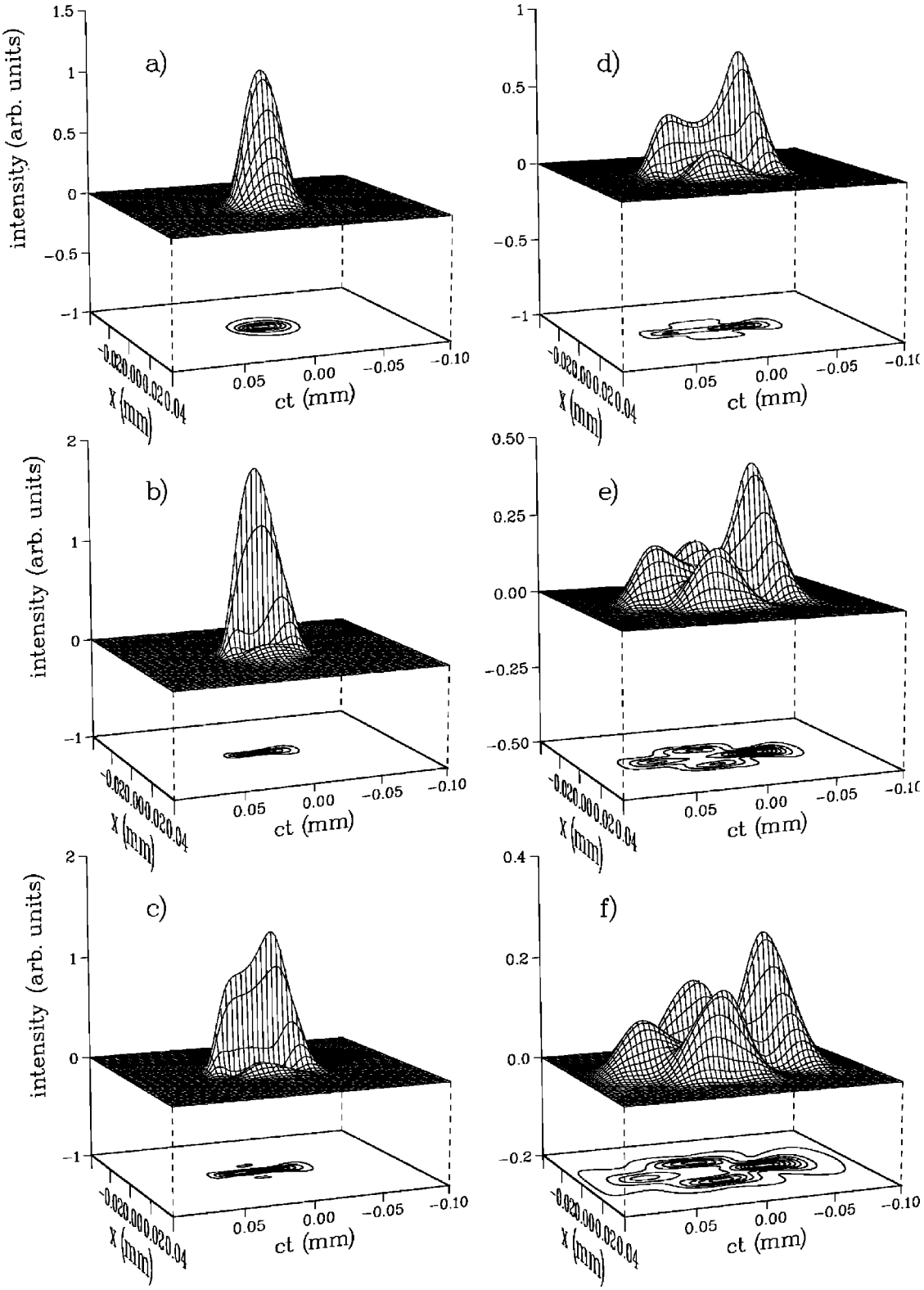

FIG. 7. Pulse intensity versus x and ct for various propagation distances L_z for a very short pulse in the normal dispersion regime (including SPM, SFS and SS). Propagation distances are the same as in Fig. 4.

$=7867\mu\text{m}<L_{\text{DSDF}}=3.23\times10^4\ \mu\text{m}<L_{\text{TOD}}=3.64\times10^4\ \mu\text{m}$. Note that DSDF (and TOD) are not entirely negligible for such a short pulse. In the series of Figs. 4–7 we show the pulse propagation dynamics as a function of propagation distance L_z in the normal dispersion regime. First we include only SPM (Fig. 4), then SPM and SS (Fig. 5), next SPM and SFS (Fig. 6), and finally we include all three nonlinear terms (Fig. 7). The maximum propagation distance shown is $L_z=3300\ \mu\text{m}$. SPM due to the nonlinear polarization is strongest at the center of the pulse (small t and x) and self-focusing results (Fig. 4). GVD spatially separates the different colors in the pulse, broadening the pulse apart in time.

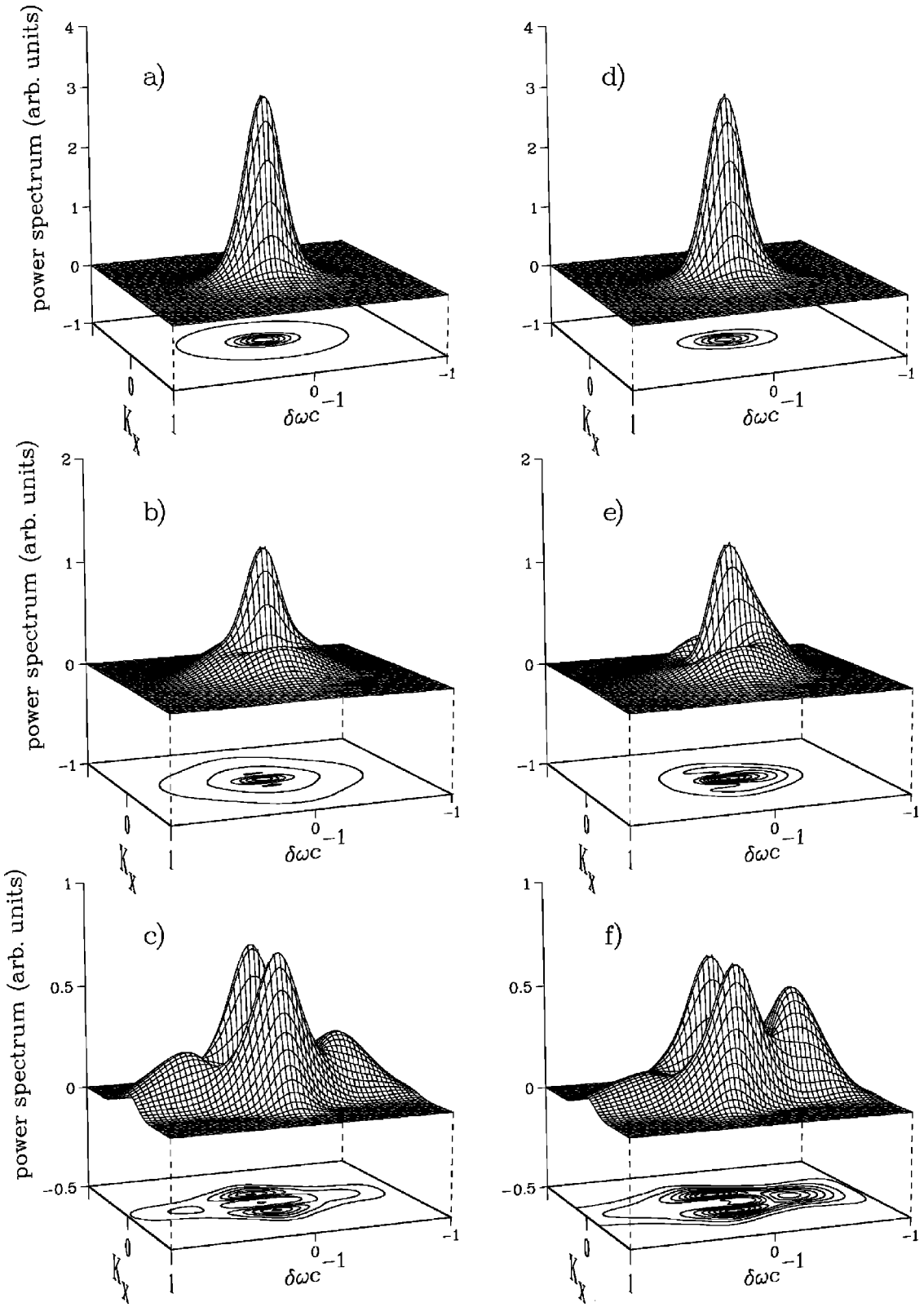

FIG. 8. Power spectra versus $\delta\omega/c=(\omega-\omega_0)/c$ and K_x. (a), (b), and (c) correspond to Figs. 4(a), 4(b), and 4(e), and (d), (e), and (f) correspond to Figs. 7(a), 7(b), and 7(f), respectively.

The pulse then breaks apart in time and forms two pulselets that are of different intensity due to the third order dispersion and the dispersion-diffraction terms [see Fig. 4(c)]. Shortly after temporal pulse splitting occurs, satellite peaks form. The two additional satellite peaks centered at $t=0$ and non-zero x are due to SPM and they are present even in the absence of SS and SFS [4] [see Figs. 4(d)–4(f)]. For pulses propagating in fibers (1D propagation) in the normal dispersion regime, SS shocks the trailing edge of the pulse and delays the peak of the pulse so that it is nearer the trailing

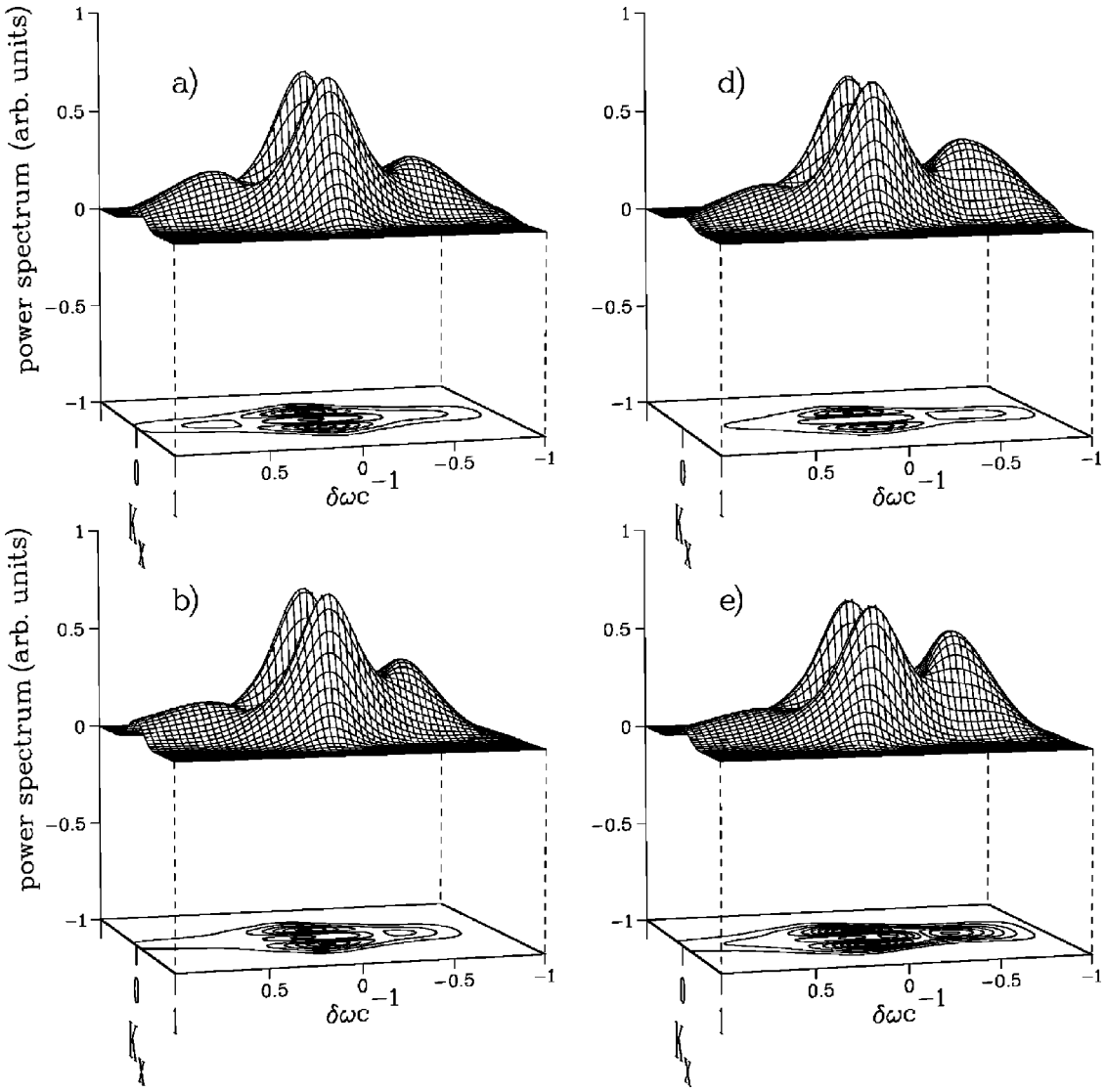

FIG. 9. Power spectra versus $\delta\omega/c=(\omega-\omega_0)/c$ and K_x with (a) only SPM, (b) SPM and SS, (9) SPM and SFS, and (d) SPM, SS, and SFS for a propagation distance of $L_z=\ldots\ \mu$m.

edge of the pulse. In contradistinction, SFS shifts the frequencies of the photons in the pulse to lower frequencies via a stimulated Raman downshifting mechanism, and the lower frequency photons have higher velocity in the normal dispersion regime. The peak of the pulse is advanced in time in comparison with the dynamics obtained by including only SPM. The SS scenario calculated here is strongly affected by dispersion. Initially, the peak of the pulse is somewhat retarded by SS, but as self-focusing at the center of the pulse develops, population shifts from the initially shocked trailing edge towards the front of the pulse, enhancing the intensity of the newly created leading pulselet [Figs. 5(c)–5(f)]. SFS enhances the leading edge of the pulse even at the beginning of the propagation [see Fig. 6(b) and compare with Figs. 4(b) and 5(b)] and enhances the leading pulselet once it has been created [Fig. 6(c)]. The enhancement of the leading edge of the pulse is due to the shifting of the frequencies towards lower frequency components by the stimulated Raman downshifting. Interplay of all the nonlinear terms further suppresses formation of the trailing pulselet, and at the same time suppresses the two off-axis satellite peaks (Fig. 7).

Figures 8(a)–8(f) show the power spectra $|A(K_x,\omega)|^2$ corresponding to Figs. 4(a), 4(b), and 4(e), and Figs. 7(a), 7(b), and 7(f) (i.e., the first three frames are without SS and SFS, and the last three are with SS and SFS). In both cases, the central peak in the Fourier domain at $\delta\omega=K_x=0$ slowly evolves first forming a pedestal [Figs. 8(b) and 8(e)] and at a later stage forming an annular ring around the central peak. Next the ring deforms as shown in Figs. 8(c) and 8(f) into the spectral features at both lower and higher frequency, and two side peaks at $K_x\neq 0$. In Fig. 9 we show the power spectra with only SPM [9(a)], SPM and SS [9(b)], SPM and SFS [9(c)], and finally SPM, SS, and SFS [9(d)] for a propagation distance of $L_z=\ldots\ \mu$m. SS sharpens the low frequency peak, and evidently broadens the high frequency component, forming a long tail at the high frequency edge. This tail is analogous to the 1D case where an ancillary frequency component to the blue of the central frequency is created [12]. SFS damps the high frequency structure, strongly enhances the low frequency structure, and moves it towards even smaller frequencies [Fig. 9(c)]. The evolution under the combined effects of SPM, SS, and SFS leads to the structure

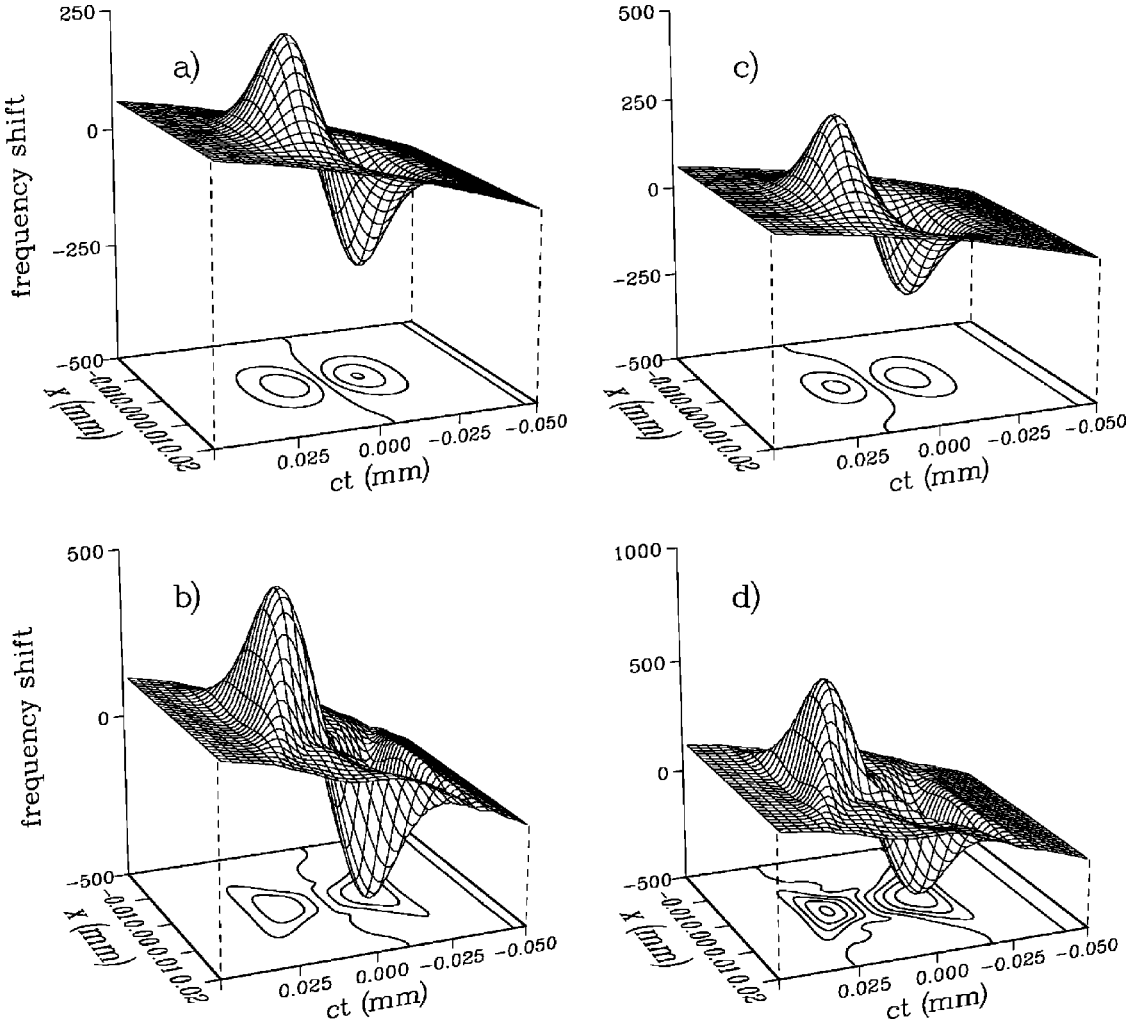

FIG. 10. $\delta\omega(\vec{x},t)$ [in units of $(\mu s)^{-1}$] vs x and ct for various propagation distances L_z in the normal dispersion regime. (a) and (b) are the local instantaneous frequency shifts corresponding to the intensities shown in Figs. 4(b) and 4(d) (without SS and SFS) and (c) and (d) correspond to Fig. 7(b), and 7(d) (with SS and SFS), respectively. The propagation distance for (a) and (c) is 1.1 mm and for (b) and (d) is 2.2 mm, respectively.

shown in Fig. 9(d), where the lower frequency structure is enhanced and dowshifted relative to Fig. 9(a), and the high frequency structure is broadened and damped relative to Fig. 9(a). This is consistent with what we see in the real space. The strongly enchanted low frequency peak in the power spectrum is detuned below central frequency ω_0 and is a counterpart of the temporarily advanced peak in real space. The peaks at finite K_x are due to self-focusing and are associated with the two additional satellite peaks in position space.

The dynamics described here are robust in the sence of generally occurring in a wide range of parameters for intense short pulses, both in the normal and anomalous dispersion regimes.

IV. OPTICAL PHASE

Additional information can be obtained by monitoring the phase $\phi(\vec{x},t)$ of the SVE defined by the equation $A(\vec{x},t) = |A(\vec{x},t)|\exp(i\phi(\vec{x},t))$. We shall plot the instantaneous local frequency shift from the central frequency ω_0, which is directly related to the optical phase. The instantaneous local frequency shift is defined as the negative of the derivative of the optical phase with respect to time [13]:

$$\delta\omega(\vec{x},t) = -\partial\phi(\vec{x},t)/\partial t = -\mathrm{Im}\left(\frac{\partial A(\vec{x},t)/\partial t}{A(\vec{x},t)}\right). \qquad (3)$$

Figure 10 shows $\delta\omega(\vec{x},t)$ vs x and ct for various propagation distances L_z in the normal dispersion regime. The results with [Figs. 10(a) and 10(b)] and without SFS and SS [Figs. 10(c) and 10(d)] show the linear frequency chirp due to GVD and the nonlinear chirp arising due to the self-phase modulation. The increase of the (almost-linear) frequency chirp with increasing propagation distance is clearly evident in the results both with and without SFS and SS. The nonlinear chirp shifts the frequencies at the forward edge of the pulse to lower frequencies and the backward edge to higher frequencies. The increase of the chirp due to SPM with propagation distance is also evident. SFS shifts the frequencies in the leading edge of the pulse to even lower values [i.e.,

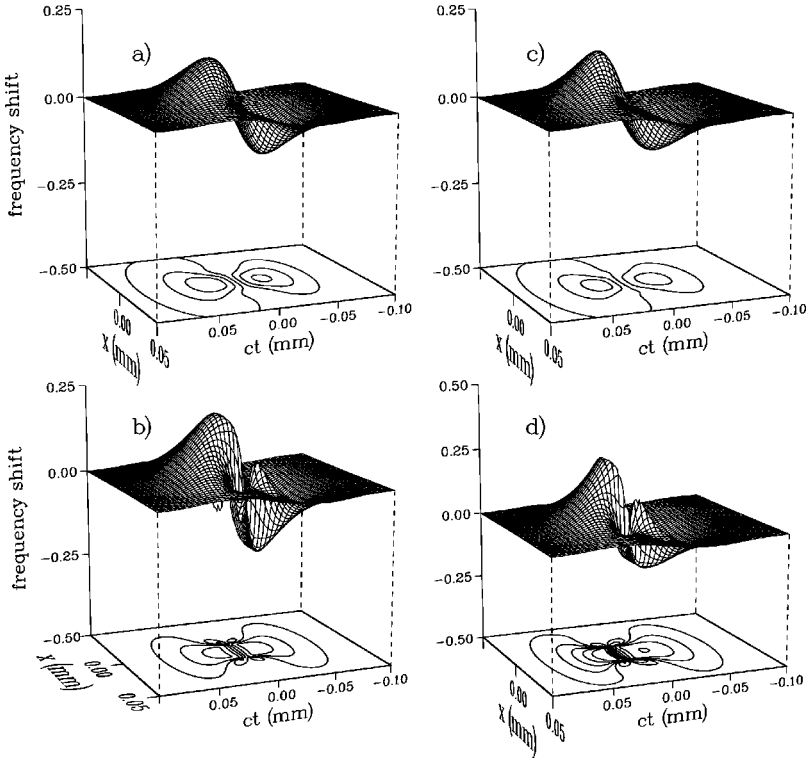

FIG. 11. $\delta\omega(\vec{x},t)$ [in units of $(\mu s)^{-1}$] vs x and ct for various propagation distances L_z in the anomalous dispersion regime. (a) and (b) are the local instantaneous frequency shifts corresponding to the intensities shown in Figs. 2(b) and 2(d) (without SS and SFS) and (c) and (d) correspond to Fig. 1(b) and 1(d) (with SS and SFS), respectively. The propagation distance for (a) and (c) is 4.1 mm and for (b) and (d) is 7.5 mm, respectively.

$\delta\omega(\vec{x},t)$ becomes more negative at the leading edge of the pulse], although this is difficult to see from the perspective in the figure, and SS changes $\delta\omega(\vec{x},t)$ at the trailing edge of the pulse so as to be more positive there. This results in a steepening of the pulse at the trailing edge. Figure 11 is similar to Fig. 10, except for the anomalous dispersion regime. Here, GVD is of opposite sign relative to Fig. 10, and the GVD is relatively weaker than the chirp due to SPM, and is therefore difficult to see in the figure. The nonlinear chirp shifts the frequencies at the forward edge of the pulse to lower frequencies and the backward edge to higher frequencies. The sharp ancillary features in the frequency chirp evident in both Figs. 11(b) and 11(d) (easiest to see in the contour plots) are not present initially but begin to gradually develop as the propagation proceeds. These features are associated with the pulse breakup process.

V. CONCLUSIONS

To summarize, we have shown how self-steepening and self-frequency shifting can affect pulse propagation dynamics, both in the normal but especially in the anomalous dispersion regimes. In the anomalous dispersion regime, the trailing edge of the pulse becomes more intense due to SFS and is shocked due to SS, and pulse breakup is strongly suppressed. In the normal dispersion regime, SFS shifts the frequency of the pulse to lower frequencies, and these lower frequencies travel faster, thus enhancing the intensity of the leading pulselet.

ACKNOWLEDGMENTS

This work was supported in part by grants from the U.S.–Israel Binational Science Foundation and the Israel Academy of Science.

[1] Y. Silberberg, Opt. Lett. **15**, 1282 (1992).
[2] J. E. Rothenberg, Opt. Lett. **17**, 583 (1992); **17,** 1340 (1992).
[3] P. B. Corkum, C. Rolland, and T. Srinivasan-Rao, Phys. Rev. Lett. **57**, 2268 (1986); P. B. Corkum and C. Rolland, IEEE J. Quantum Electron. **25**, 2634 (1989).
[4] M. Trippenbach and Y. B. Band, Phys. Rev. A **56**, 4242 (1997).
[5] G. P. Agrawal, *Nonlinear Fiber Optics* (Academic Press, New York, 1989); M. Gedalin, T. C. Scott, and Y. B. Band, Phys. Rev. Lett. **78**, 448 (1997).
[6] F. DeMartini, C. H. Townes, T. K. Gustafson, and P. L. Kelly, Phys. Rev. **164**, 312 (1967); T. K. Gustafson, J. P. Taran, H. A. Haus, J. R. Lifsitz, and P. L. Kelly, *ibid.* **177**, 306 (1969).
[7] D. Grischkowsky, E. Courtens, and J. A. Armstrong, Phys. Rev. Lett. **31**, 422 (1973).
[8] J. R. de Oliveira, M. A. de Moura, J. M. Hickmann, and A. S.

L. Gomes, J. Opt. Soc. Am. B **9**, 2025 (1992).

[9] Y. B. Band and M. Trippenbach, Phys. Rev. Lett. **76**, 1457 (1996).

[10] M. Trippenbach, T. C. Scott, and Y. B. Band, Opt. Lett. **22**, 579 (1997).

[11] M. Trippenbach and Y. B. Band, J. Opt. Soc. Am. B **13**, 1403 (1996); C. Radzewicz, J. S. Krasinski, M. J. la Grone, M. Trippenbach, and Y. B. Band, *ibid.* **14**, 420 (1997).

[12] W. H. Knox, R. L. Fork, M. C. Downer, R. H. Stolen, and C. V. Shank, Appl. Phys. Lett. **46**, 1120 (1985).

[13] One might also consider the phase $\Phi(\vec{x},t)$ defined by $A(\vec{K},\omega)=|A(\vec{K},\omega)|\exp(i\Phi(\vec{K},\omega))$, where by analogy it is clear that

$$\partial\Phi(\vec{K},\omega)/\partial\omega=\mathrm{Im}\left(\frac{\partial A(\vec{K},\omega)/\partial\omega}{A(\vec{K},\omega)}\right).$$

We shall not present any numerical results for this quantity.